Inorganica Chimica Acta, 49 (1981) 37–45
©Elsevier Sequoia S.A., Lausanne – Printed in Switzerland

Ligand Bonding Parameters in some Macrocyclic, Seven-Coordinate Complexes of Nickel(II) and Cobalt(II)

MALCOLM GERLOCH and LYALL R. HANTON
University Chemical Laboratories, Lensfield Road, Cambridge CB2 1EW, U.K.

Received September 18, 1980

Single crystal polarized electronic spectra and paramagnetic susceptibilities throughout the temperature range 20–300 K are reported for the complexes $[M(H_2O)_2(tdmmb)][BF_4]_2$; *M = Ni(II), Co(II); tdmmb = 7,15-dihydro-7,9,13,15-tetramethylpyrido-[2′,1′,6′:12,13,14][1,2,4,7,9,10,13]-heptaazacyclo-pentadeca[3,4,5,6,7,8-*aklmn*][1,10]phenanthroline. The electronic properties of these formally pentagonal bipyramidal macrocyclic complexes are analysed within a global, axial model – shown to be wholely inappropriate for the nickel complex – and within the angular overlap model. The ligand fields are dominated by the phenanthroline-type ligator as a strong σ donor and π donor, presumably reflecting the presence of electron rich nitrogen atoms substituted in the phenanthroline* ortho *positions. By contrast the two imine groups of the macrocycle act as weak σ donors in line with the much longer M–N bond lengths. Despite the ligand field asymmetry in the macrocycle plane, the molecular magnetic susceptibility tensor is calculated to be essentially axial with respect to the normal to this plane.*

Introduction

As part of a programme of macrocyclic coordination chemistry in this laboratory, Lewis, O'Donoghue and Ramsden [1, 2] have synthesised complexes of various transition metal ions with macrocycles which incorporate either phenanthroline or bipyridine. The present study of magnetic and spectral properties, requiring large single crystals of each complex, concerns two such systems, $[M(H_2O)_2(tdmmb)][BF_4]_2$; M = Ni(II), Co(II), where tdmmb is the macrocycle (1) involving formal phenanthroline, imine and pyridine-type ligators.

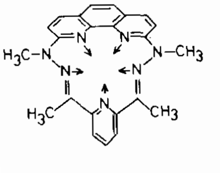
(1)

Crystal structure analyses [3–5] of both complexes have demonstrated an approximate coplanarity for the macrocycle (even more exact when the methyl substituents are replaced by hydrogen [6]) and a formal pentagonal bipyramidal coordination geometry for the complex cations as a whole. The patterns of bond lengths involving the donor nitrogen atoms suggest that there is no extensive π delocalization network throughout the macrocycle. The same conclusion has been reached [4] from qualitative comparisons of ultraviolet spectra from many related complexes, from NMR studies and, to some extent, from electrochemical reduction studies of the complexed ligand. Ramsden [4] has also suggested that the electronic properties of the phenanthroline moiety are likely to be substantially modified by the *ortho* substituted nitrogen groups, his conclusions being based particularly on the pattern of metal–nitrogen bond lengths observed in these and related molecules.

In this study, we have measured the principal paramagnetic susceptibilities of both the nickel and cobalt complexes as single crystals throughout the temperature range 20–300 K, and crystal, polarized electronic absorption spectra. The data are analysed within two models. In the first, we examine the applicability of a global view of the complexes as of essentially D_{5h} symmetry, and in the second, we use the angular overlap model and try to define the separate bonding roles of the individual ligators in the coordination shell. The molecules bear some resemblance to those involving the planar, pentacoordinate chelate, dapsc (2) which have been the subject of a similar study [7, 8].

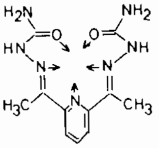
(2)

Experimental

The complexes, diaqua(7,15-dihydro-7,9,13,15-tetramethylpyrido[2′,1′,6′:12,13,14] [1,2,4,7,9,10,

TABLE I. $[Ni(tdmmb)(H_2O)_2](BF_4)_2$: Interpolated Experimental Principal Crystal Susceptibilities (cgsu × 10^4) and Mean Moments.

T/K	χ_1	χ_2	χ_3	$\bar{\mu}$/B.M.
25	423	507	397	2.97
35	310	356	301	3.00
55	207	228	200	3.05
75	155	167	150	3.07
95	122	129	119	3.06
115	101	107	100	3.07
135	86	91	86	3.08
155	75	79	76	3.08
175	66	70	68	3.08
195	60	63	61	3.09
215	55	57	56	3.10
235	50	52	51	3.10
255	47	48	47	3.11
275	43	45	44	3.11
295	41	41	42	3.12

TABLE II. $[Co(tdmmb)(H_2O)_2](BF_4)_2$: Interpolated Experimental Principal Crystal Susceptibilities (cgsu × 10^4) and Mean Moments.

T/K	χ_1	χ_2	χ_3	μ/B.M.
25	212	976	890	3.72
35	183	740	677	3.86
55	159	494	453	4.03
75	143	363	336	4.10
95	127	281	263	4.12
115	113	230	215	4.14
135	102	194	182	4.15
155	92	168	158	4.16
175	84	149	140	4.17
195	77	133	125	4.17
215	71	120	113	4.17
235	66	110	104	4.19
255	62	101	95	4.19
275	58	94	88	4.19
295	54	88	82	4.20

13]-heptaazacyclopentadeca[3,4,5,6,7,8-*aklmn*] [1, 10]phenanthroline)-nickel(II) and -cobalt(II) bis-(tetrafluoroborate), $[M(H_2O)_2(tdmmb)][BF_4]_2$, were prepared [4] by Dr. J. Ramsden, to whom we are grateful for pure, powdered samples. Recrystallization of freshly filtered hot solutions in water with excess sodium fluoroborate yielded, on slow cooling for 2–3 days, large, single crystals of the complexes suitable for spectroscopic and magnetic measurements.

Susceptibility measurements were made on crystals weighing between 1 and 2 mg. The nickel and cobalt complexes are isomorphous, with monoclinic crystal symmetry [3, 5]. For each complex, using our single crystal Faraday balance and procedures described elsewhere [9], we measured:

(*1*), χ_1 and χ_2 for crystals oriented parallel to *b*,

(*2*), χ_b and $\chi_{c'}$ for crystals oriented parallel to *a*, and

(3) χ_b and $\chi_{a'}$ for crystals oriented parallel to *c*. The duplicate measurements of χ_b from different crystals agreed to better than 2% throughout the experimental temprature range 20–300 K. By observation of the setting angle of the crystals in the *ac* plane the angle ϕ, defined from $\chi_1(<\chi_2)$ to *a*, measured from the positive crystal *a* axis through the positive *c* axis, was found to be –65° for the nickel crystals and +38° for the cobalt ones. Additionally, ϕ was deduced from the relationships

$$\sin^2(\beta - 90 - \phi) = (\chi_{a'} - \chi_1)/(\chi_2 - \chi_1) \qquad (1)$$

and

$$\sin^2\phi = (\chi_{c'} - \chi_2)/(\chi_1 - \chi_2) \qquad (2)$$

which gave ϕ values ranging –55 to –65° for the nickel complex and +31 to +42° for the cobalt one. The various methods are substantially in agreement, in view (a) of the experimental difficulty in observing ϕ directly and (b) of the relationships (1) and (2) involving the ratios of differences between observables. We estimate that the ϕ angles vary by less than 5° throughout the temperature range. In Tables I and II we list interpolated, experimental principal crystal susceptibilities for the nickel and cobalt complexes, for which a diamagnetic correction χ_M^{dia} = 273 × 10^{-6} cgsu (1 cgsu ≡ $4\pi \times 10^6$ m^3 mol^{-1}) has been applied.

Electronic absorption spectra have been recorded throughout the range 4000 to 20000 cm^{-1} using Cary 17D spectrophotometer. [Spectra in the U.V. range are reported by Ramsden]. As for the seven-coordinate dapsc complexes [7, 8], spectral resolution is poor and not much improved on lowering the temperature to *ca.* 5K. In Figures 1 and 2 are shown spectra for crystals with light incident of the *bc* plane, polarized parallel and perpendicular to the unique crystal axis. The value of these polarized spectra (as opposed to unpolarized) appears to be in increasing confidence in the presence of adsorption at *H*5000 cm^{-1} for the nickel complex and at *ca.* 5100 cm^{-1} for the cobalt one. Rather similar features at *ca.* 5000 cm^{-1} for the nickel complex and at *ca.* spectra of both cobalt and nickel complexes. They are weak and poorly resolved: the most convincing evidence of their reality as *d–d*, spin-allowed bands derives from their subsequent analysis within the angular overlap model. The small feature at *ca.* 14,970 cm^{-1} in the cobalt spectrum is presumably due to a spin-forbidden transition.

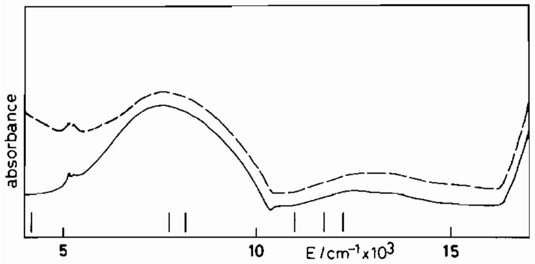

Fig. 1. $[Ni(H_2O)_2(tdmmb)][BF_4]_2$: Polarized single-crystal transmission spectra for light incident on the *bc* plane at *ca.* 300 K. Markers correspond to spin-triplets calculated with parameter set B of Table IV.

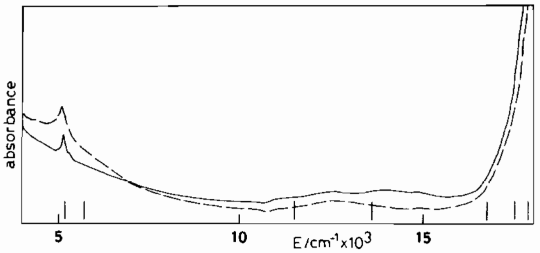

Fig. 2. $[Co(H_2O)_2(tdmmb)][BF_4]_2$: Polarized single-crystal transmission spectra for light incident on the *bc* plane at *ca.* 300 K. Markers correspond to spin-quartets calculated with the parameter set in Table IV.

Ligand Field Analyses

(a) The Nickel(II) Complex

We have available complete, single-crystal paramagnetic susceptibilities of the nickel(II) macrocycle complex throughout the temperature range 20–300 K. Our analysis initially relies heavily upon these data in view of the relatively uninformative electronic spectra discussed earlier. An analysis within the angular overlap model is expected to pose problems of the resolution of individual ligand parameters in these highly coordinated complexes and will have almost no value if the ligand field describes an essentially pentagonal bipyramidal molecular coordination. Our first step, therefore, was to attempt to reproduce the crystal paramagnetism in this system within such an axial model using a global parameterization scheme. The orbital ordering within such a D_{5h} symmetry model is expected to be $d_{z^2} > d_{xy}, d_{x^2-y^2} > d_{xz}, d_{yz}$; the z axis being oriented perpendicular to the plane of the macrocycle. Only two ligand field parameters are required to define this situation, $\epsilon(z^2)$ and $\epsilon(xy)$, referring to the energies of the z^2 and $xy/x^2 - y^2$ orbitals relative to the xz, yz pair. As the d_{xz}, d_{yz} metal functions interact only with out-of-plane macrocycle π orbitals and the axial water π orbitals, the D_{5h} model can only yield appropriate *differences* between σ and π bonding effects in the complex. However, within this scheme we have calculated [10] crystal magnetism for the nickel(II) compound, for $\epsilon(z^2)$ and $\epsilon(xy)$ values lying in the range 4000 to 20,000 cm^{-1} with the interelectron repulsion, Racah B parameter held at 700 cm^{-1}, and for the spin–orbit coupling coefficient ζ allowed to vary between 100 and 600 cm^{-1}. None of these circumstances permit even a qualitative reproduction of the observed magnetic properties. Typically, calculated crystal susceptibilities are 180,000; 16,000; 5,000 (cgsu × 10^{-6}), at 20 K, as compared with the observed values 51,000; 40,000; 42,000. Thus, a consideration of the single-crystal paramagnetism alone, unambiguously precludes a description of the ligand field in this complex as axially symmetric with respect to the normal to the macrocycle plane. A generalized departure from the axial model requires the parameterization of all orbital energies *and* of off-diagonal matrix elements of the ligand field within that orbital basis. Accordingly, we turned next to the angular overlap model [11, 10].

Representation of the ligand field within the a.o.m. for these complexes requires the parameter list: e_σ, $e_{\pi\perp}$, $e_{\pi\parallel}$ for each of the three chemically distinct nitrogen donors of the macrocycle – phenanthroline, imine and pyridine types – where ⊥ and ‖ refer to out-of and in-plane π bonding; e_σ and e_π for the axial water ligands (in view of the non-location of the hydrogen atoms of these water molecules in the X-ray structure analysis and the usual uncertainty of the nominal hybridization state of the donor oxygen atom, we presume an average cylindrical metal–water π interaction); the Racah B, spin–orbit ζ, and Stevens orbital reduction k factors. Several considerations preclude the possibility of establishing values for all these parameters. The consequences of holohedrized symmetry [12] mean that several a.o.m. parameters will be correlated to a greater or lesser degree: for example, the d_{xz} and d_{yz} metal orbitals (z taken normal to the macrocycle here) interact with both the water π functions and the various out-of-plane macrocycle π functions, so that we must expect considerable difficulty in distinguishing these different perturbations: similarly, the d_{xy} or $d_{x^2-y^2}$ orbitals are affected by all of the σ orbitals on the macrocycle donor groups. Finally, the paucity of the spectral information available describes an insufficiently exacting criterion for so heavily parameterized a model. We have used our confidence in the a.o.m. approach, [13–15] therefore, to reduce the degree of parameterization in line with chemical intuition. In addition to the approximation of the 'linearly ligating' axial water ligands discussed above, we have presumed zero π bonding from all nitrogen ligators in the plane of the macrocycle. The remaining a.o.m. parameter set then comprises e_σ(phen), e_σ(imine),

TABLE III. Coordination Bond Lengths (A) in $[M(H_2O)_2(tdmmb)][BF_4]_2$.

M	Phen	Imine	Pyridine	Water
Cobalt	2.11 2.12	2.25 2.23	2.10	2.18 2.18
Nickel	2.10 2.08	2.31 2.28	2.12	2.10 2.08

e_σ(py), $e_{\pi\perp}$(phen), $e_{\pi\perp}$(imine), $e_{\pi\perp}$(py), $e_\sigma(H_2O)$, $e_\pi(H_2O)$. As the analysis progressed, we were able to remove several more of these e parameters from the list of variables.

The first priority was to reproduce the crystal magnetism. Initially we were guided in the choice of the relative magnitudes of the e_σ parameters by consideration of the coordination bond lengths given in Table III, associating larger e_σ values with the shorter nickel–nitrogen bond lengths of the phenanthroline and pyridine-type donors and smaller ones with the long nickel–imine bonds. *Pro tem*, and having in mind the idea that the earlier axial model should be some approximation to the true situation, we set all e_π parameters to zero; that is, initially doubting that we could dinstinguish the π bonding parameters amongst themselves. This strategy immediately revealed that a marked improvement in reproducing the magnetic behaviour is possible. The calculated magnetism is a sensitive function of the differences between the various e_σ parameters, figures of merit (see refs. 10, 14) for the agreement with experiment ranging 0 to 100%. Good magnetic fits are achieved only for parameter sets involving large values of e_σ(phen) and much smaller e_σ values for all other ligators. Attempts to ignore the experimental pattern of coordination bond lengths, such that low e_σ(phen) values were associated with various other high e_σ values, all failed to give even qualitative reproduction of the experimental paramagnetism. At this stage, therefore, there emerged the certain conclusion, again based on the crystal magnetism, that the ligand field is described in terms of a dominant σ donor role for the phenanthroline-type ligators.

Attempts to refine our description the ligand field are based on the simultaneous reproduction of the crystal magnetism and spectra. The spectrum may be summarised as comprising a band ν_1 at <5,000 cm^{-1}, a large absorption ν_2 at 7,500 cm^{-1}, a weaker and uncertain feature ν_3 at *ca.* 12,500 cm^{-1}, and the onset of more intense absorptions ν_4 at energies >17,500 cm^{-1}. The last feature is unresolved and quite probably is to be assigned to charge-transfer transitions. The shoulder at *ca.* 18,000 cm^{-1} may or may not reveal a *d–d* transition. We presume that all components of the $^3F \rightarrow {}^3P$ manifold lie in this region and our calculations have all been made by adjusting the Racah *B* parameter to place $\rightarrow {}^3P$ components within this high-energy envelope. As some uncertainty attaches to the feature ν_3, we enquired whether it is possible to calculate all components of ^3F within the ν_2 band or at lower energies. However, any choice of a.o.m. parameters placing all ^3F components below *ca.* 9,000 cm^{-1}, also places the first excited state within 2,000 cm^{-1} of the ground state. Satisfactory reproduction of the crystal magnetism empirically requires this energy gap to be $\gtrsim$3,000 cm^{-1}. Accordingly, the refinement process involves placing the first calculated excited state between 3,000 and 5,000 cm^{-1}, the next two centred under the large absorption at *ca.* 7,500 cm^{-1}, and the highest three ^3F components together associated with ν_3 avoiding the experimentally transparent region at 10,000 to 11,000 cm^{-1}. In the present coordination geometry and with wide ranges of all e parameters, no other pattern of spectral assignments is possible with the simultaneous reproduction of the crystal magnetic susceptibilities.

In optimising the whole parameter set we observe the following features and trends: (*i*) for variations of e_σ(py) in the range 2,500 to 4,500 cm^{-1}, most components of the ^3F manifold are little affected; the most sensitive is the first excited state whose calculated energy decreases by *ca.* 400 cm^{-1} as e_σ(py) increases by 1,000 cm^{-1}; (*ii*) the first excited state is also depressed, by *ca.* 800 cm^{-1}, for an increase in e_σ(imine) of 1,000 cm^{-1} when this parameter lies in the range 2,000 to 3,500 cm^{-1}; the next two levels increase by only 300 to 400 cm^{-1} for a similar change in e_σ(imine) and the remaining components of ^3F are little affected; (*iii*) all components of ^3F are sensitive to variations in e_σ(phen) within the range 4,500 to 6,500 cm^{-1}; a change from 5,500 cm^{-1} to 6,500 cm^{-1}, increases the calculated energy of the first excited state by *ca.* 1,200 cm^{-1}, of the next two by *ca.* 900 cm^{-1} and of the remainder by *ca.* 1,200 cm^{-1}; (*iv*) within the range e_σ(water), 3,000 to 4,500 cm^{-1}, the calculated energy of the first excited state is constant while the remaining ^3F levels increase by *ca.* 1,000 to 1,500 cm^{-1}; (*v*) the first excited state is unaffected by changes in $e_{\pi\perp}$(py), $e_{\pi\perp}$(imine), $e_{\pi\perp}$(phen) or e_π(water); general shifts in the other two groups of ^3F levels are observed with some level crossing within (but not between) levels in each group; thus the highest lying five components of ^3F shift upwards in energy by *ca.* 1,000 cm^{-1} for an increase of 500 cm^{-1} in e_π (water), of 1,000 cm^{-1} in $e_{\pi\perp}$(phen), of 750 cm^{-1} in $e_{\pi\perp}$(imine), and are essentially unaffected by $e_{\pi\perp}$(py).

In summary of these trends, we note that satisfactory reproduction of the magnetism, requiring the

TABLE IV. Summary of Optimal Parameter Sets; Energies in cm^{-1}.

Parameter[a]	Nickel Complex		Cobalt Complex
	A	B	
e_σ(phen)	6,500	6,000	5,000
$e_{\pi\perp}$(phen)	1,000	1,500	1,000
e_σ(imine)	2,500	2,500	3,000
e_σ(py)	3,500	3,500	4,000
e_σ(water)	3,800	3,800	3,500
e_π(water)	1,500	1,100	1,000
B	700	700	700
ζ	300	300	520
k	0.8	0.8	0.6

[a] Values for $e_{\pi\perp}$(imine), $e_{\pi\perp}$(py), $e_{\pi\parallel}$(macrocycle) are all set to zero for both complexes, see text.

first excited state to be at least 3,000 cm^{-1} from ground, is most affected by e_σ(py), e_σ(imine) and e_σ(phen). In particular, that level is increased in energy by increasing e_σ(phen) or by decreasing e_σ(py) and/or e_σ(imine). In Table IV, we list two sets of parameters we consider to yield equally best reproduction of both spectral and magnetic properties of this nickel complex. We are unable to define the uniqueness of these fits beyond the trends given in the preceding paragraph and to note that all a.o.m. values are probably determined within ±500 cm^{-1}, given that the sets in Table IV were selected after attempting to keep all e_σ values as similar as possible, and all e_π values as small as possible. More extreme disparity between e_σ values, for example, may permit acceptable fit to the observed properties, but we have not investigated possibilities for any e_σ outside the range 2,000 to 6,500 cm^{-1}. Further, we have set $e_{\pi\perp}$(py) to zero in view of (ν) above, and $e_{\pi\perp}$(imine) to zero in view of the long nickel–nitrogen bond lengths: in any case, the correlation between these values and those for e_π(water) essentially precludes any clear resolution between these three features. Altogether, therefore, while noting that the e_π values listed in Table IV reproduce the various experimental data, we prefer merely to note that the phenanthroline-type ligator and the water molecules both act as moderately good π donors towards the central metal. Table V lists the calculated eigenvalues corresponding to the representative 'best fit' parameter set B given in Table IV, while comparison between observed and calculated crystal susceptibilities is shown in Fig. 3. The calculated monoclinic angle ϕ is −59°, comparing well with the experimental values of −55 to −65°, given above. The ground triplet term suffers a zero-field splitting such that levels are calculated to lie at 0, 2 and 10 cm^{-1}.

TABLE V. Comparison between Observed Transition Energies and Eigenvalues Calculated with the Parameter Set B in Table IV for [Ni(H$_2$O)$_2$(tdmmb)][BF$_4$]$_2$: Energies (cm^{-1}) Averaged over Spin-triplets.

Calculated	Observed
20,833	>17,500
20,427	
18,580	
12,213	12,500
11,692	
10,899	
8,145	7,500
7,741	
4,146	<5,000
0	

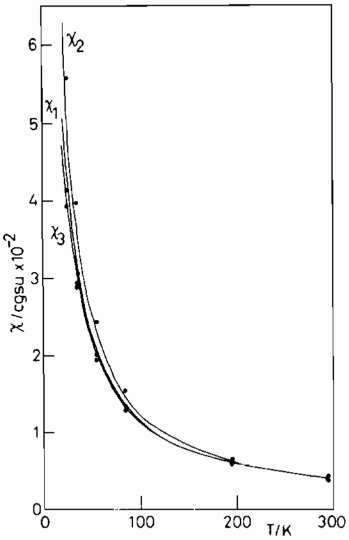

Fig. 3. Comparison of observed and calculated (circles) crystal susceptibilities for [Ni(H$_2$O)$_2$(tdmmb)][BF$_4$]$_2$: parameters from set B of Table IV.

Corresponding to the optimal a.o.m. parameters in Table IV, we have computed the equivalent d^1 orbital energies. These are, for set A: 0,671; 1,954, 6,731; 9,434 cm^{-1}: and for set B; 0, 1,018; 2,367, 6,535; 9,623 cm^{-1}. In each case the energies relate to orbitals described predominantly as $xz, yz; x^2 - y^2$ and xy; z^2, respectively. It is interesting to compare this orbital splitting pattern with the e_1'', e_2', a_1' levels of the idealized D_{5h} scheme. The e_1'' levels, xz and yz are split by only 600 to 1,000 cm^{-1} and are nearly pure in the model parameterized in Table IV, while the e_2' levels, xy and $x^2 - y^2$ are split by 4,500 to 5,000 cm^{-1} and are mixed together. This behaviour of the xy and $x^2 - y^2$ orbitals clearly reflects the large difference between the e_σ value of

TABLE VI. $[Ni(H_2O)_2(tdmmb)][BF_4]_2$: Calculated Molecular Susceptibilities at 25 K corresponding to the Parameter set B in Table IV.

Principal Susceptibilities (cgsu × 10^4)		Orientation[a]		
		X	Y	Z
K_1	390	166.2°	91.5	76.2
K_2	420	76.2	91.2	13.9
K_3	574	91.2	1.9	88.5

[a]Orientation of molecular frame [Y perpendicular to macrocyle; Z parallel to Ni–N(py)] with respect to orthogonal crystal frame is given by the direction cosines:

	a	b	c'
X	0.2303	0.7317	−0.6416
Y	−0.8060	−0.2260	−0.5471
Z	−0.5453	0.6431	0.5377

TABLE VII. Comparison between Observed Transition Energies and Eigenvalues Calculated with the Parameter Set in Table IV for $[Co(H_2O)_2(tdmmb)][BF_4]_2$: Energies (cm^{-1}) Averaged over Spin Quartets.

Calculated	Observed
17,831 17,481 16,682	>17,000
13,650 11,493	12,500
5,713 5,165	5,100
3,450	
2,651	
0	

the phenanthroline-type ligators and the rest; and the mixing is such that the diagonalized orbitals in the real nickel(II) complex tend to orient towards the phenanthroline-type nitrogen donor atoms.

Finally, it is interesting to note the characteristics of the calculated *molecular* susceptibility tensor corresponding to these 'best fit' parameter sets. These are illustrated in Table VI for one such optimized parameter set, at 25 K. We observe that the molecular magnetism is essentially axial *with respect to the normal to the macrocycle.* Thus, despite the large $xy/x^2 - y^2$ orbital energy splitting and inequality of the various e_σ parameters, the molecular magnetism apparently reflects the pentagonal bipyramidal coordination geometry more than the dominant σ and π donor roles of the phenanthroline-type ligands. We consider this little more than a curio, however, for the very large anisotropy calculated in our initial axial model has been steadily reduced by the increasing in-plane, ligand field anisotropy together with a decreasing difference between total, molecular axial and equatorial field strength. No doubt an even greater value for e_σ(phen) would ultimately remove the effective five-fold axis and select the pseudo-two-fold axis passing through the pyridine as a dominant magnetic direction.

(b) The Cobalt(II) Complex

As for the d^8 complex, we have available complete susceptibility data from single crystals of the cobalt complex throughout the temperature range 20–300 K. The cobalt crystals are more anisotropic than the nickel ones. Once more, sparse spectral information ultimately limits the sensitivity of the present analysis. Despite having demonstrated a dominant role for the phenanthroline-type ligators in the nickel complex, we began our analysis of the cobalt system, as with the nickel, by investigating the utility of a simple axial, D_{5h}, model in reproducing the crystal magnetism. With the Racah B parameter held at 700 cm^{-1} and ζ varying between 300 and 520 cm^{-1}, we considered orbital energies $\epsilon(z^2)$ and $\epsilon(xy)$ throughout wide ranges. Unlike the situation for the nickel complex, however, excellent reproduction of the crystal susceptibilities is possible in this model for ζ = 520 cm^{-1}, $\epsilon(xy)$ 4,000 to 6,000 cm^{-1}, and $\epsilon(z^2)$ 8,000 to 10,000 cm^{-1}. For the lower limits – $\epsilon(xy)$ = 4,000 cm^{-1} and $\epsilon(z^2)$ = 8,000 cm^{-1} – transitions are calculated within the spectral range to lie at about 4,800; 10,600 to 11,700; and 16,100 cm^{-1} and higher. At the upper limits of 6,000 and 10,000 cm^{-1} for $\epsilon(xy)$ and $\epsilon(z^2)$, respectively, calculated transitions are placed in the region, 4,600 to 6,500 cm^{-1} and at 14,400 cm^{-1} and beyond. Neither eigenvalue set accords well with the (poorly) observed spectral maximum at 5,100; 12,500 to 13,500 cm^{-1}; and >17,000 cm^{-1}. Nevertheless, an acceptable reproduction of the observed spectrum should be possible with a choice of $\epsilon(xy)$ and $\epsilon(z^2)$ parameters intermediate between these extremes, so that a description of the ligand field of the cobalt complex as axially symmetric with respect to the macrocycle plane is not incompatible with the experimental data.

In view of a similar statement for the nickel complex being quite wrong, however, we have also tested the response of the a.o.m. parameterization in the cobalt species. An identical a.o.m. parameter set to that used in the nickel analogue yields rather poor agreement with the crystal magnetism. We note, however, that the inequality of metal–nitrogen bond lengths in the coordination shell of the cobalt molecules is less than in the nickel, so we chose a para-

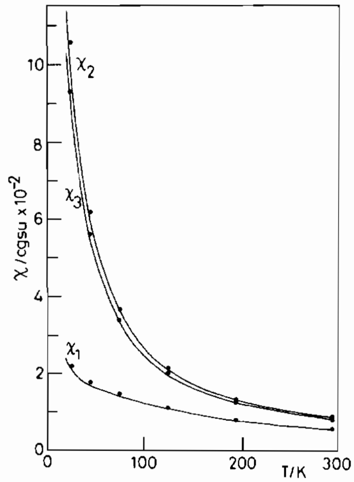

Fig. 4. Comparison of observed and calculated (circles) crystal susceptibilities for $[Co(H_2O)_2(tdmmb)][BF_4]_2$: parameters from Table IV.

meter set which was similar to the optimal one for the nickel system but with a much less dominant σ donor role for the phenanthroline-type ligator. The parameter set given in Table IV yields excellent reproduction of the crystal magnetism and a satisfactory description of the spectrum, given in Table VII. In view of the adequacy of the axial model, however, this parameter set cannot be described as 'unique'. It corresponds to a subjective choice, reflecting the pattern of coordination bond lengths between the two molecules and the parameter sets for the nickel complex. Within the local region of parameter space, however, we note that an e_σ(phen) value of 4,500 cm^{-1} is equally acceptable but that e_σ(imine) 3,500 or e_π(imine) –500 cm^{-1} both yield significantly less satisfactory spectral and magnetic properties.

Corresponding to the 'best fit' parameter set in Table IV and eigenvalues in Table VII, are shown the calculated crystal susceptibilities in Fig. 4. The corresponding zero-field splitting in 64 cm^{-1}. The calculated monoclinic setting angle ϕ is *ca.* 33° compared with the mean observed value of 36°. The corresponding molecular susceptibility tensor is approximately axial with $K_\perp < K_\parallel$, details being summarised, at the representative temperature 25K, in Table VIII. The one-electron or orbital energies corresponding to these properties are 0,690; 3,794, 5,870; 9,367 cm^{-1} for xz, yz; $x^2 - y^2$, xy; and z^2, respectively. We note a similar splitting of the xz, yz orbital pair to that in the nickel complex, determined, of course, by the similar π parameterization; but a substantially smaller separation of the $x^2 - y^2$ and xy functions reflecting the less dominant role of the phenanthroline-type ligand in the cobalt complex.

TABLE VIII. $[Co(H_2O)_2(tdmmb)][BF_4]_2$: Calculated Molecular Susceptibilities at 25 K Corresponding to the Parameter Set in Table IV.

Principal Susceptibilities (cgsu × 10^4)		Orientation[a]		
		X	Y	Z
K_1	177	90.0	0.5	89.5
K_2	968	56.2	90.5	33.8
K_3	1063	33.8	89.8	123.8

[a] Orientation of molecular frame [Y perpendicular to macrocycle; Z parallel to Co–N(py)] with respect to orthogonal crystal frame is given by the direction cosines:

	a	*b*	*c'*
X	0.2172	0.7202	–0.6589
Y	–0.8155	–0.2371	–0.5280
Z	–0.5365	0.6520	0.5358

Discussion

The ligand field analyses just presented rely on well-defined crystal susceptibility data and on disappointing and ill-resolved crystal spectra. Further, the high coordination of the metal atoms in these species together with the effects of holohedrized symmetry provide severe circumstances for the angular overlap model. Our analyses have been presented in some detail in order to convince the reader that the maximum bonding information has been obtained without undue over-parameterization. The situation in the nickel complex is the more clearly defined. The magnetic properties established a dominant role for the phenanthroline-type ligand moiety as a σ donor and, in conjunction with the spectrum, as a significant π donor also. A description of the total ligand field of approximately axial symmetry is not appropriate. The magnetic and spectral properties of the cobalt system can be reproduced adequately by either a global axial model or by a local potential model (a.o.m.) similar to that in the nickel complex but with a similar σ-donor role for the phenanthroline-type groups. In both systems, the calculated molecular susceptibility tensors are roughly axial with respect to the macrocycle plane; this, despite the clearly non-axial nature of the ligand field in the nickel complex. For comparison we have completed the molecular magnetic properties of the corresponding iron(II) complex [2], using similar parameter values to those in the cobalt system with a range of e parameters for the water ligands (the Fe–water bond lengths are *ca.* 0.03 Å longer than for Co–water) and for various ζ values. The molecular susceptibility tensor is once more approximately axial with respect to the macrocycle plane, with '$K_{\parallel}$' > '$K_{\perp}$'.

The short length of the metal–phenanthroline bonds observed in these complexes obviously correlates well with the large magnitude of the a.o.m. e parameters established in the present study. The phenanthroline moiety acts as a donor in both σ and π bonding modes, however. This could occasion some surprise, perhaps, in that the well-known function of phenanthroline and related ligands to stabilize transition metals in low oxidation states would involve a π acceptor role. Certainly, such has been demonstrated recently [13] in terms of a negative e_π parameter for biquinoline within a tetrahedrally coordinated nickel(II) system. Further, a consideration of the electroneutrality principle and synergic back-bonding might also suggest that strong σ-donation from a ligand should be associated with strong π-acceptance by it. It is clear, however, that the phenanthroline moiety does not behave in this characteristic fashion in the present species, not least in that the pale yellow colour of the nickel complex, or pale orange of the cobalt, contrast with the intense colours of most comparable, phenanthroline-containing complexes. Instead, the characteristic ligand group in these molecules is the moiety (3), in which we presume the *ortho*, formally sp^2, non-coordinating nitrogen groups donate negative charge to the phenanthroline. It is interesting to compare this with the situation [7] in the complex Co(dapsc)(H$_2$O)$_2$ in which the *keto* groups, in positions corresponding to the phenanthroline groups here, act as especially good π donors despite their intrinsically poor σ donor qualities. In that system the $>$C=O → moiety is coordinated to both –NH and NH$_2$ groups in the semicarbazone.

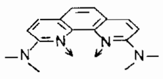
(3)

While an essentially electrically neutral state for the phenanthroline group may be achieved in its role as electron conductor from the peripheral nitrogens to the central metal, a similar neutrality for the metal appears to require a correspondingly diminished acceptor property from several or all of the remaining ligand groups. The long metal–imine bond lengths and small e_σ(imine) a.o.m. parameter both appear to suggest that only a relatively weak interaction exists between the metal and these groups. Both pieces of data were responsible for our *choice* that e_π(imine) is zero. In further support is the expectation that the otherwise anticipated π acceptor role for these imine groups should be diminished by the same peripheral nitrogen groups responsible for modifying the π bonding character of the phenanthroline group. In view of the evidence against an extended delocalization throughout the macrocycle, we presume the electronic effects of the periferal nitrogens to be one of a general polarization of negative charge onto surrounding groups with the result of a qualitative trend in these neighbouring groups towards more positive e parameters in general.

Both spectroscopic and magnetic properties in these two complexes are rather insensitive to the parameterization of the pyridine groups, especially with respect to π bonding, so that parameter values for these ligators given in Table IV should be regarded as illustrative only.

While the σ role of the axial water molecules is established only approximately, the analysis of the nickel complex indicates a significant degree of π donation which, for reasons discussed above, was presumed to be cylindrical in nature. In some degree, the extensive correlation between $e_{\pi\perp}$ values of the macrocycle and e_π(H$_2$O) inhibits a clear discrimination between these various π bonding roles, so that the large e_π(H$_2$O) value may in part be an artefact of the model. However, we note that a broad absorption [4] in the infrared spectrum of these complexes crystallized, as here, with the fluoroborate counterion suggests a significant degree of hydrogen bonding in the lattice: fairly close O····F contacts observed in the crystal structure support this (in contrast the infrared spectrum [4] of the corresponding salts with PF$_6^-$ indicate a much smaller degree of hydrogen bonding). In that any such hydrogen bonding would enhance contributions to the metal–water bonding from metal–hydroxy-like structures, a larger value for e_π(H$_2$O) may have further significance.

Finally, it is worth noting that, despite the very large value chosen for e_σ(phen) in the nickel system, for example, that the mean e_σ in the complex is about 4,100 cm^{-1} and the mean e_π about +570 cm^{-1}. As an example, in a sense, of the law of average environment [12], these figures suggest that a similar degree of electric neutrality of the ligands appears to occur, regardless of the metal coordination number: and that the same is probably true of the central metal after one takes the different coordination geometries as well as different coordination numbers into account.

Acknowledgements

We thank the Royal Society, London, for a Rutherford Scholarship and the New Zealand University Grants Committee for financial support (to L.R.H.). We are grateful to Dr. J. Ramsden for samples of these complexes and for helpful discussions. Finally, we thank Rank Xerox for the loan of the Cary 17D spectrophotometer.

References

1 J. Lewis, T. D. O'Donoghue and P. R. Raithby, *J. Chem. Soc. Dalton Trans.*, 1383 (1980).

2 M. M. Bishop, J. Lewis, T. D. O'Donoghue, P. R. Raithby and J. N. Ramsden, *J. Chem. Soc. Dalton Trans.*, 1390 (1980).

3 J. Lewis, P. R. Raithby and J. N. Ramsden, in preparation.

4 J. N. Ramsden, *Ph.D. Thesis, Cambridge University* (1980).

5 L. R. Hanton and P. R. Raithby, *Acta Cryst., B36*, 1489 (1980).

6 C. W. G. Ansell and P. R. Raithby, unpublished results.

7 M. Gerloch, I. Morgenstern-Badarau and J.-P. Audière, *Inorg. Chem., 18*, 3220 (1979).

8 M. Gerloch and I. Morgenstern-Badarau, *Inorg. Chem., 18*, 3225 (1979).

9 D. A. Cruse and M. Gerloch, *J. Chem. Soc. Dalton Trans.*, 152 (1977).

10 'CAMMAG', a FORTRAN computer program by D. A. Cruse, J. E. Davies, J. H. Harding, M. Gerloch, D. J. Mackey and R. F. McMeeking.

11 C. E. Schäffer, *Structure and Bonding, 5*, 68 (1968), and references therein.

12 C. K. Jørgensen, 'Modern Aspects of Ligand Field Theory', North-Holland, Amsterdam (1971).

13 M. Gerloch, L. R. Hanton and M. R. Manning, *Inorg. Chim. Acta, 48*, 205 (1981).

14 R. G. Woolley, *Mol. Phys.*, in press.

15 M. Gerloch, J. H. Harding and R. G. Woolley, *Structure and Bonding*, in press.

16 M. Gerloch, R. F. McMeeking and A. M. White, *J. Chem. Soc. Dalton Trans.*, 2452 (1976).